JOURNAL OF APPLIED ELECTROCHEMISTRY **27** (1997) 543–549

Flexible synthesis of mixed metal oxides illustrated for $LiMn_2O_4$ and $LiCoO_2$

D. G. FAUTEUX, A. MASSUCCO, J. SHI

Hirion Electrochemical Inc., Acorn Park, Cambridge, MA 02140, USA

C. LAMPE-ÖNNERUD

Massachusetts Institute of Technology, 77 Massachusetts Avenue, Cambridge, MA 02139, USA

Received 30 October 1995; revised 15 July 1996

A new dynamic process (DP) for rapid and continuous mixed metal oxide synthesis is illustrated for $LiMn_2O_4$ and $LiCoO_2$. The DP synthetic method offers the possibility of producing pure or mixed lithiated metal oxide materials of controlled composition, phase-content, particle size, porosity and morphology. The final metal oxides are made from low-cost reactants; metals, carbonates and acetic acid, and are well suited for industrial scale-up. Characterization includes XRD, SEM, TEM, TGA, BJH (Barrett, Joyner, Halendal), laser beam light diffraction and electrochemical measurements. The DP synthesis method may offer high quality electrode materials (with total pore areas of 76 $m^2\ g^{-1}$) to the future battery industry as scale-up is easily adopted.

1. Introduction

Cathode materials containing a lithiated transition metal oxide have received intense research efforts as to their prospective use in secondary high energy density lithium ion batteries. Four volt cathode material candidates, which have been studied for more than ten years, include both $LiMn_2O_4$ [1–9] and $LiCoO_2$ [9–17] synthesized in several different ways. The solid state synthesis route using a lithium compound, typically Li_2CO_3, $LiNO_3$, $LiOH.xH_2O$, or Li_2O as the lithium source is the most commonly used [5, 11–14]. For the synthesis of $LiMn_2O_4$, MnO_2 is almost exclusively used as the manganese source, whereas reactions using cobalt metal, Co_3O_4 or $CoCO_3$ as the source of cobalt for the synthesis of $LiCoO_2$ have been reported . Solid state synthesis processes are normally carried out in air and include several heat treatments in the temperature range of 600 to 900 °C, each followed by a particle size reduction step. To obtain phase-pure reaction products, the synthesis often takes several days.

There are also reports on solid state $LiMnO_2$ synthesis under argon, where carbon black was used as the reducing agent (see e.g., [18]). The synthesis of $LiMn_2O_4$ using reactive electron beam evaporation [3] and RF magnetron sputter deposition [7], followed by some post annealing to form the spinel structure have been reported for the production of thin electrodes showing future possibilities for the fabrication of very thin batteries. The results of several studies on lithiated transition metal oxide synthesis from liquid media have been reported. This approach offers low-temperature synthesis with excellent product homogeneity. $LiMn_2O_4$ has also been synthesized under reduced pressure using citrate precursors and metal nitrates [4]. Gels of $LiMn_2O_4$ have been formed from the reduction of aqueous permanganate solutions, $H_{0.5}Li_{0.5}MnO_4$, by fumaric acid [2]. In basic solution, both the $LiMn_2O_4$ spinel and the layered $LiCoO_2$ have successfully been prepared from acetate precursors [9].

In this work we describe a dynamic process (DP) synthesis method enabling the rapid and continuous synthesis of pure and mixed lithiated metal oxides with controlled composition, particle size, morphology, porosity and crystallinity. This flexible process is illustrated for the synthesis of $LiMn_2O_4$ and $LiCoO_2$. A brief description is also included for other mixed lithiated metal oxides which have been made using the same DP synthesis method. Some of the initial electrochemical behaviour characterization results of the cathode materials produced were previously reported [19]. The emphasis of this report is on the synthesis and characterization of the DP produced $LiMn_2O_4$ and $LiCoO_2$.

2. Synthesis

The DP synthesis method developed is based on the continuous generation of an airborne aerosol of lithiated metal oxide precursors in solution in a carrier solvent, followed by a high temperature solid state reaction, and the collection of the produced lithiated metal oxide particles. The experimental setup can be seen in Fig. 1.

The first step of the process, the generation of an airborne aerosol of the lithiated metal oxide precursors, is accomplished using a Sonotec® ultrasonic atomizer nozzle (3.5 W/120 kHz). Compressed air

0021-891X

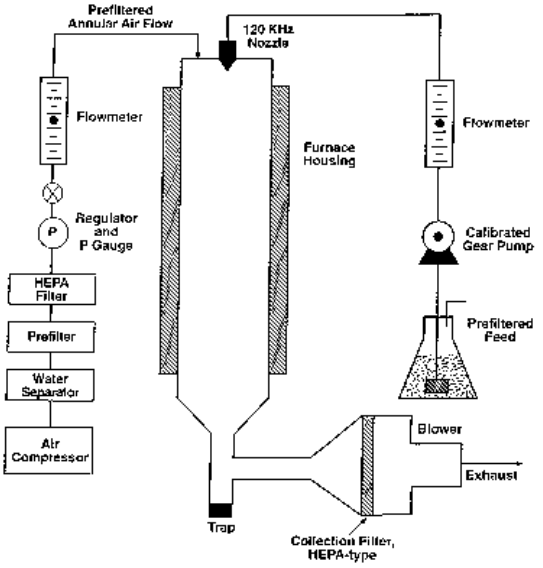

Fig. 1. Schematic overview of the experimental setup for synthesis of lithiated mixed metal oxides using the dynamic process (DP) method.

(ambient), filtered through an air–water separator, a prefilter, and a HEPA type glass fibre filter (Gelman A/E), was used as a carrier gas at a flow rate of $20\,L\,min^{-1}$. This atomizer was selected because of its capability of producing 'wet' droplets of the lithiated metal oxide precursor solution (feed solution) of approximately $20\,\mu m$ average diameter. The interrelationship between the feed solution concentration, viscosity, surface tension, the atomizer power and frequency of operation, determine the aerosol 'wet' droplet size, throughput, and the final 'dry' lithiated metal oxide particle size. Operating conditions can be established for the proposed DP synthesis method which can yield an optimum throughput.

Typically 10 to 25 wt% of lithiated metal oxide precursor feed solutions were used for the DP synthesis. These solutions were prepared by dissolving metal salts; $LiCH_3COO.2H_2O$ (FMC, 99.9%), and $Mn(CH_3COO)_2.4H_2O$ (Barker, reagent) or $Co(CH_3COO)_2.4H_2O$ (Barker, reagent), respectively in distilled water. The solutions were filtered (Whatman, no.6) to avoid problems with the metering gear pump.

The second step of the DP synthesis involves the evaporation of the solvent and the chemical reactions to form the final lithiated metal oxides. The rate of evaporation of the carrier solvent was varied to characterize its effect on the final morphology and topography of the particles produced. The solvent evaporation and chemical reactions took place in a 2 m vertical Inconel (alloy 600, schedule 40) three temperature zone tube furnace (inner diameter 0.07 m) kept at temperatures ranging from 100 °C to 1000 °C. The temperature in each zone of the tube furnace was varied in order to establish the best synthesis condition for $LiMn_2O_4$ and $LiCoO_2$. The results presented in the following used a temperature of 750 °C in all three zones. The total residence time in the furnace for the chemicals was 2–3 s. This residence time was controlled by adjusting the air flow through the tube furnace using an air blower exhaust (BGI, GBM-2000H) located behind the glass filter discussed in the following paragraph. In addition to controlling the residence time, the air blower exhaust produces a small negative pressure (3 kPa) in the system, thus avoiding any leakage of small particles or gases to the surrounding atmosphere.

The third step of the DP synthesis method is the collection of the particles. In the current experimental set-up (Fig. 1), the powder particles were collected on a 20 cm × 25 cm glass fibre filter (HEPA, Gelman A/E) at a temperature above 140 °C in order to avoid any condensation of water. To ensure a complete conversion, a post heat treatment for 5 min. at 750 °C was applied in a separate furnace just prior to use. This ensures complete conversion and dryness. Ball milling (Szegavari Attritor 1S) was used to further decrease the particle size of the DP produced $LiMO_x$ materials. The resulting particle size distribution of the $LiMO_x$ was measured using a laser beam light diffraction technique (Microtrac FRA) as a function of grinding time.

3. Characterization

Thermogravimetric analysis (TGA) measurements were carried out on the DP synthesis method precursor solution using a TA Instrument 2050 under dry air (Airco, dry grade) at atmospheric pressure. The sample was initially heated to 750 °C at rate of $2\,°C\,min^{-1}$, then maintained at 750 °C for 8 h and thereafter heated ($2\,°C\,min^{-1}$) to 950 °C. Intermediate reaction products heated at $2\,°C\,min^{-1}$ were analysed for phase purity and degree of crystallinity after air quenching from 150 °C and 400 °C, respectively. All DP- and commercially-produced samples ($LiMn_2O_4$ from Cyprus Foote (99.4%)); $LiCoO_2$ from FMC (battery grade) were characterized in terms of phase and degree of crystallinity by powder X-ray diffraction (XRD) using a Rigaku RU300 diffractometer (CuK_α radiation). For the final products step-scans covering 5.00°–120.00° in steps of 0.03° in 2θ were collected and structure refinements were performed using the Rietveld method [20] implemented in the computer program GSAS [21]. The morphology and grain size of the samples were studied with a Cambridge S200 scanning electron microscope (SEM) and a Topcon 002B transmission electron microscope (TEM). Porosimetry measurements using mercury intrusion (AutoPore II 9220) were also performed.

4. Results and discussion

The mechanistic study of the reported DP synthesis method shows that the formation of $LiMn_2O_4$ and $LiCoO_2$ occurs through a successive set of similar reaction steps. The first reaction step for the synthesis of both the $LiMn_2O_4$ and $LiCoO_2$ involves the evaporation of the solvent from the metal oxide

precursor solutions. To this step corresponds the largest sample weight loss, as observed in the TGA curve (Fig. 2). In the case of the manganese oxide synthesis reaction sequence, subsequent to the solvent evaporation, the presence of crystalline $Mn(CH_3COO)_2.4H_2O$ is identified with XRD, for samples collected at 150 °C. However, at this temperature no lithium-containing phase can be identified, suggesting that the lithium species are mainly amorphous. In the case of the cobalt oxide synthesis reaction sequence, subsequent to the solvent evaporation the sample is completely amorphous at a temperature of 150 °C. It is possible by controlling the temperature and duration of evaporation to greatly vary the density of the produced particle. It is also during the solvent evaporation step that the size of the agglomerate and of the metal oxide crystallites are defined.

The second reaction step in the synthesis reaction sequence of both the $LiMn_2O_4$ and $LiCoO_2$ begins at temperatures as low as 240 °C and corresponds to the formation of Li_2CO_3 and to the formation of a binary metal oxide mixture of M(+II) and M(+IV); i.e. $MnO + Mn_3O_4$ and $CoO + Co_3O_4$, respectively. Already at a temperature as low as 400 °C, the desired phases of the $LiMn_2O_4$ and $LiCoO_2$ can be identified with XRD. However, the samples are not fully converted. As the temperature reaches 750 °C, only the desired phase of the lithiated metal oxides, $LiMn_2O_4$ and $LiCoO_2$, can be identified using XRD.

The main reaction steps involved in the DP synthesis of lithiated metal oxide compounds are the evaporation of the solvent followed by the reaction of the acetates to form the metal oxides. The DP synthesis reaction steps involved during the production of the lithium manganese oxide can be summarized as follows:

$$4\,LiCH_3COO.2H_2O + 8\,Mn(CH_3COO)_2.4H_2O + 43\,O_2 \rightarrow 4\,LiMn_2O_4 + 40\,CO_2 + 70\,H_2O \quad (1)$$

The corresponding DP synthesis reaction steps involved during the production of the lithium cobalt oxide are

$$4\,LiCH_3COO.2H_2O + 4\,Co(CH_3COO)_2.4H_2O + 25\,O_2 \rightarrow 4\,LiCoO_2 + 24\,CO_2 + 42\,H_2O \quad (2)$$

In addition to identifying the major lithiated metal oxide synthesis reaction steps, TGA results revealed smaller but continuous weight changes over the entire temperature range up to 950 °C in both the $LiMn_2O_4$ and $LiCoO_2$ systems. In the case of the synthesis of the lithium manganese oxide material , the sample weight reaches a maximum at 750 °C. However, if the sample is held isothermally at 750 °C for an extensive period of time (~ 8 h) the sample loses weight, suggesting a slight loss of oxygen and the formation of $LiMn_2O_{4+x}$. This loss of oxygen is temperature dependent and was recently shown to be reversible when the temperature is lowered [22]. XRD reveals the formation of amorphous components in samples synthesized under these conditions. A different temperature and time dependence is found during synthesis of the lithium cobalt oxide, in which the maximum sample weight is found at the end of the 8 h isothermal hold at 750 °C. This indicates a slower uptake of oxygen to form the final $LiCoO_2$ compared to the reaction mechanism of the lithium manganese metal oxide. As the temperature is raised to 950 °C both samples decompose. Thus, by using the DP synthesis method it is possible to tailor the oxygen content of the lithium metal oxides by varying the temperature and the reaction/annealing time.

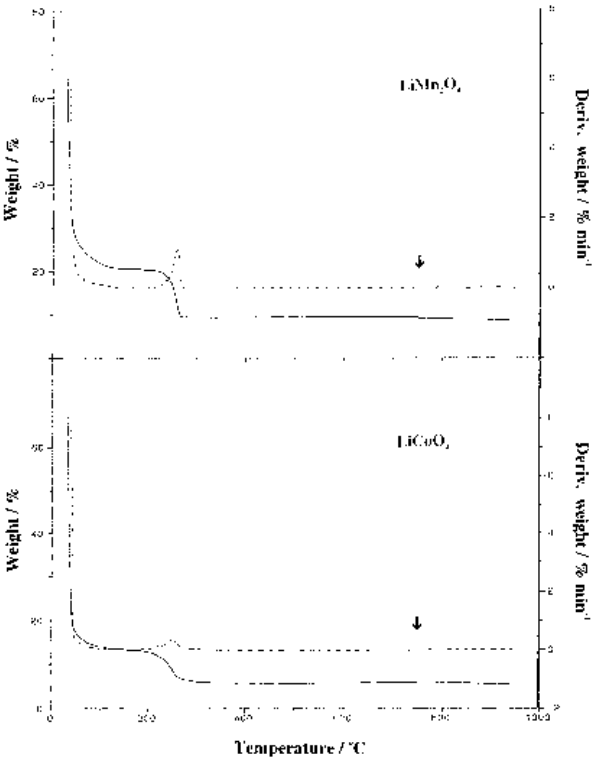

Fig. 2. TGA (2 °C min^{-1}) for the formation of $LiMn_2O_4$ and $LiCoO_2$ from their acetate precursors. The arrow indicates the isothermal hold at 750 °C for 8 h.

The $LiMn_2O_4$ and $LiCoO_2$ products made using the DP synthesis method show high crystallinity and well defined powder grains. This was unexpected considering the short residence time in the reaction furnace of 2–3 s, and the short post-annealing period of 5 min or less. The Rietveld refinements (Fig. 3) of the as-made final products of $LiMn_2O_4$ and $LiCoO_2$ show a remarkable agreement with crystallographic data previously reported for $LiMn_2O_4$ [23, 24] and $LiCoO_2$ [25]. For both cases of the DP-produced lithiated metal oxides, the crystal unit cell parameters were slightly smaller than the unit cell parameters reported in the literature. It can be speculated, based on the TGA results, that these differences may depend on some oxygen deficiencies. Cell parameters, atomic positions, thermal displacement parameters and final agreement factors are summarized in Table 1.

The resulting morphology of the DP produced lithiated metal oxides exhibit rather large powder particles (Fig. 4 (a) and (b)) defined by a porous shell

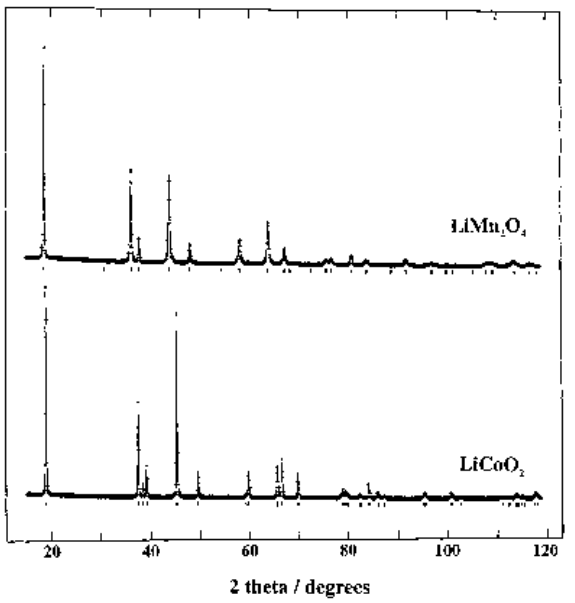

Fig. 3. X-ray (CuK_α) diffraction patterns of $LiMn_2O_4$ and $LiCoO_2$ made by the DP synthetic route. The figure includes observed (dotted line) diffractogram, calculated Rietveld (solid line) pattern and tic-marks for the respective phase.

(Fig. 4 (c) and (d)). However, TEM analysis on $LiMn_2O_4$ made by the DP synthesis method, reveals that the powder grains consist of small ~30 nm crystallites (Fig. 5). Results indicating improved electrochemical reversibility of the DP-$LiMn_2O_4$ in comparison to commercial products were previously reported [19]. This behaviour was attributed to the small crystallite sizes. The flexibility of the DP synthesis method, with regard to powder porosity, was proved by varying the feed solution concentrations and the precursor droplet sizes. The high poro-sity of the DP powder particles was confirmed by BJH (Barrett, Joyner, Halendal) (Fig. 6) measurements showing a maximum total intrusion volume of 4.20 mL g^{-1}, which can be compared with 0.856 mL g^{-1} for the commercial sample. The maximum total pore area obtained for the DP-$LiMn_2O_4$ was measured to 76.3 $m^2 g^{-1}$ and the bulk density to 0.226 g cm^{-3} the commercial sample measured 9.92 $m^2 g^{-1}$ and 1.20 g cm^{-3}, respectively.

Particle size reduction through ball milling and grinding (attrition) represent an important and energy consuming processing step in the preparation of electrode components for batteries. It is well known that transition metal oxides, such as $LiMn_2O_4$ and $LiCoO_2$, are rather hard and abrasive materials, which consequently adds to the complexity of the particle size reduction process. An advantage of the DP synthesis method is the flexibility to directly produce different particle sizes and to vary the morphology of the particles. This can be achieved by using variable operating parameters such as different feed solution concentrations, droplet sizes, solvents and carrier gas flow rates. The morphology of the $LiMn_2O_4$ and $LiCoO_2$ particles as produced using the DP synthesis method, has proven to be beneficial to further particle size reductions. As the microscopy analysis illustrates, each of the DP produced lithium metal oxide small particles is an aggregate of crystallites loosely held together. Knowing that the cohesive force between the crystallites forming the aggregate is much less than the force within the crystal lattice, it is evident that the energy dispersed during the particle size reduction process can be efficiently used to break down these larger aggregates into their smaller crystalline constituent. This was confirmed by the particle size distribution analysis as a function of grinding time (Fig. 7). Longer grinding time is needed to reduce the size for commercial samples compared to DP produced samples. For example, the $LiCoO_2$, made according to the DP synthesis method reported here, had after 100 min of ball-milling reached a maximum particle size of less than 10 μm compared to the 1100 min needed for the $LiCoO_2$ commercial sample to reach the same maximum particle size value.

By using the DP synthetic method, several lithiated mixed metal oxide compounds with different compositions can be made. For example, we have

Table 1. Crystallographic data for as made DP $LiMn_2O_4$ and $LiCoO_2$ obtained from Rietveld refinements

Phase	*$LiMn_2O_4$*		*$LiCoO_2$*	
Space group	*Fd3m* *Li: 8a, Mn: 16d, O: 32e*		*R-3m* *Li: 3b, Co: 3a, O: 3c*	
	This work	*References* [23] *and* [24]	*This work*	*References* [25]
Cell / pm	$a = 824.03(3)$	$a = 824.76(2)$	$a = 281.512(7)$ $c = 1405.42(5)$	$a = 281.66$ $c = 1405.2$
Atomic position	O: $x = 25.58(2)$	O:$x = 26.1(2)$	O: $z = 25.59(1)$	O:$z = 26$(-)
Thermal parameters / $(nm)^2$	$B_{Li} = 0.3(3)$ $B_{Mn} = 1.03(4)$ $B_o = 2.28(8)$	$B_{Li} = 0.5$(-) $B_{Mn} = 0.3(2)$ $B_o = 0.4$(-)	$B_{Li} = 1.2(2)$ $B_{Co} = 0.76(3)$ $B_o = 1.00(6)$	(non reported)
Agreement factors / %	$Rp = 7.32$ $Rwp = 9.99$	$Rp = 3.6$ $Rwp = 4.0$	$Rp = 6.84$ $Rwp = 8.77$	(not reported)

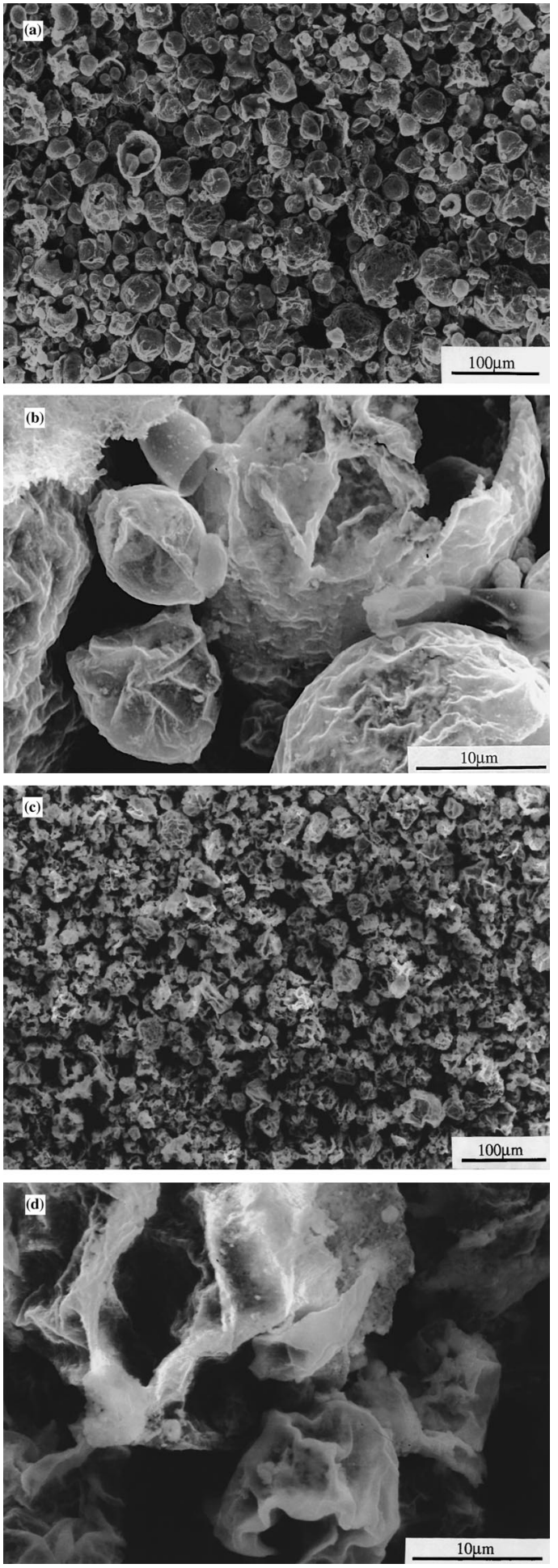

Fig. 4. SEM pictures of as-made DP $LiMn_2O_4$ (a) and (b) and of DP $LiCoO_2$ (c) and (d).

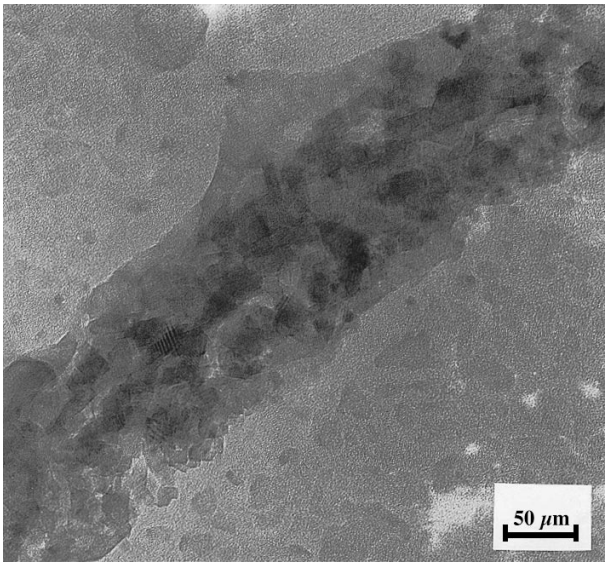

Fig. 5. TEM on $LiMn_2O_4$ showing the as-made $LiMn_2O_4$ crystallites synthesized by the DP synthesis method.

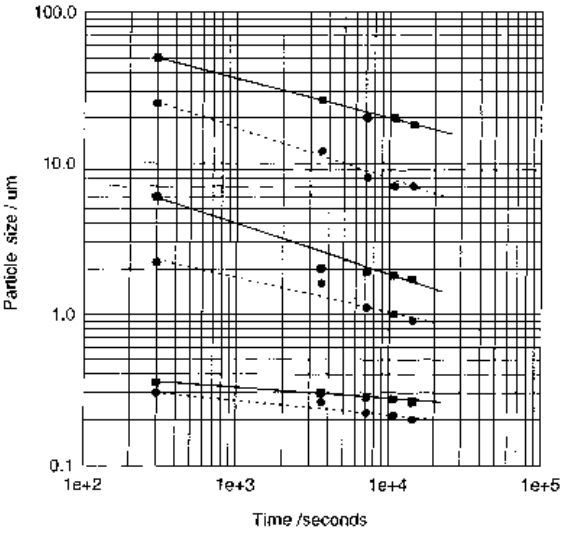

Fig. 7. Results from ball milling the DP-produced $LiCoO_2$ (●) and the commercial sample (■), including results from maximum, intermediate and minimum particle sizes.

varied the lithium content in $Li_xMn_2O_4$ for $0 < x < 2$ successfully, although some problems were encountered for higher x as the more water sensitive tetrahedral oxide forms. Phase-pure compounds were obtained for stoichiometries near $x = 1$ and $x = 2$. Small variations of the lithium content are possible without observing any phase separation. Chemically modified cathode materials offer interesting electrochemical and structural properties [26]. The processing flexibility of the DP synthesis method makes this process suitable for synthesis of doped or chemically modified electrode materials. Indeed, $LiMn_{2-y}M_yO_4$ with M = Fe, Cr, Al, Ni and Co for $y \leq 25\%$ have been produced using this DP synthesis method. In some cases, various precursors may alter the reaction mechanism and lead to some property differences of the final products. This was found in the electrochemical comparison between $LiMn_2O_4$ made from acetate and nitrate precursors [19]. A much higher capacity at 4 V for the first discharge was obtained for the acetate $LiMn_2O_4$ (110 mA h g^{-1}) compared to its equivalent nitrate synthesis (81 mA h g^{-1}). However, at 3 V the inverse relationship was found; 90 mA h g^{-1} for the acetate and 116 mA h g^{-1} for the nitrate synthesis. For comparison, the commercial $LiMn_2O_4$ reference material has a capacity of 87 mA h g^{-1} at 4 V and 58 mA h g^{-1} at 3 V.

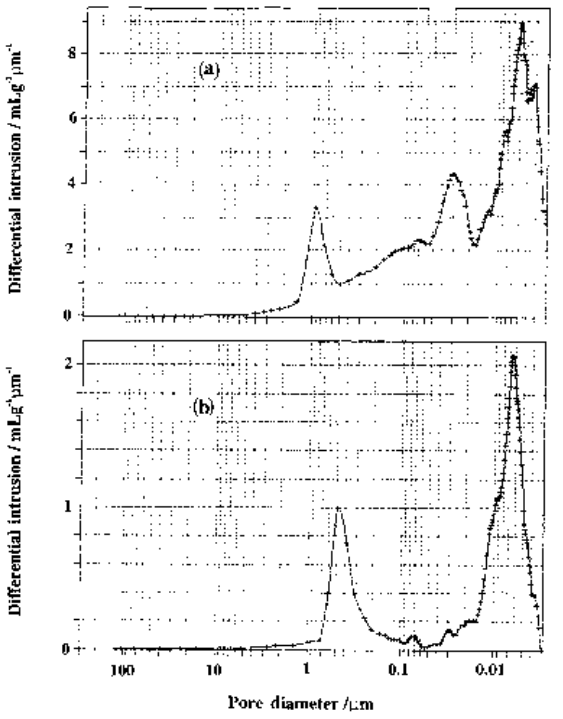

Fig. 6. Differential intrusion of Hg into (a) DP and (b) commercial $LiMn_2O_4$ samples.

5. Concluding remarks

The DP synthetic method presented and illustrated for $LiMn_2O_4$ and $LiCoO_2$ provides a possibility to produce pure or mixed lithiated metal oxide materials of *controlled* composition, phase-content, particle size, porosity and morphology rapidly. This new dynamic process can be used to prepare an array of cathode materials for use in rechargeable lithium batteries and can be summarized in three main steps; (i) the initial formation of an aerosol and the evaporation of the solvent from the precursor affecting the particle sizes, (ii) the following hetero- and homogenous chemical reactions influencing phase-content and porosity, and (iii) the final post-treatment controlling the oxygen content in the final product. The developed experimental setup is mechanically simple and process improvements such as sequential post-annealing allowing for crystallization of the cathode material can easily be implemented as the three synthesis steps can correspond to three different temperature zones in one furnace. For future energy minimization of the production of mixed metal oxides, the DP synthetic method can be used to prepare the precursor particles (steps (i) + (ii)), which

are later converted by a short heat treatment to the final products. From an energy standpoint it is also interesting to note that it is economical to produce porous large agglomerates that are easily reduced to small particles in the final milling and which can be used to mix the cathode components together. One can visualize other ways in which the flexible DP can be varied through changes in the feed stream (e.g., suspension or emulsion), gas composition (e.g., inert gas or oxygen-enriched) and temperature profile of the reactor. The DP synthesis method enables the fast and continuous production of lithiated metal oxides made from low-cost reactants (such as metals, carbonates and acetic acid) is well suited for industrial scale up, and will provide high quality electrode materials to the battery industry.

Acknowledgements

This work has been supported in part by ORD (93F-151600–000). We are also indebted to Dr M. Rona and Dr J. Sigalovsky for generous assistance.

References

[1] M. M. Thackeray, W. I. F. David, P. G. Bruce and J. B. Goodenough, *Mat. Res. Bull.* **18** (1983) 461.
[2] S. Bach, J. P. Pereira-Ramos, N. Baffier and R. Messina, *Electrochim. Acta* **37** (1992) 1301.
[3] F. K. Shokoohi, J. M. Tarascon, B. J. Wilkens, D. Guyomard and C. C. Chang, *J. Electrochem. Soc.* **139** (1992) 1845.
[4] M. Sugawara, M. Fujiwara and K. Matsuki, *Prog. Batteries Battery Mater.* **12** (1993) 181.
[5] A. Momchilov, V. Manev, A. Nassalevska and A. Kozawa, *J. Power Sources* **41** (1993) 305.
[6] W. F. Howard, Proc. 7th Lithium Battery Meeting, **IA35** (1994) 281.
[7] H. Huang and P. G. Bruce, *J. Electrochem. Soc.* **141** (1994) L76.
[8] J. Barker, K. West, Y. Sajdi, R. Pynenburg, B. Zachau-Christensen and R. Koksbang, *J. Power Sources* **54** (1995) 4759.
[9] P. Barboux, J. M. Tarascon and F. K. Shokoohi, *J. Solid State Chem.* **94** (1991) 185.
[10] A. Mendiboure, C. Delmas and P. Hagenmuller, *Mat. Res. Bull.* **19** (1984) 1383.
[11] K. Mizushima, P. C. Jones, J. P. Wiseman and J. B. Goodenough, *ibid.* **15** (1980) 783.
[12] M. G. S. R. Thomas, P. G. Bruce and J. B. Goodenough, *J. Electrochem. Soc.* **132** (1985) 1521.
[13] M. Yoshio, H. Tanaka, K. Tominaga and H. Noguchi, *J. Power Sources* **40** (1992) 347.
[14] J. N. Reimers, J. R. Dahn and U. von Sacken, *J. Electrochem. Soc.* **140** (1993) 2752.
[15] J. R. Dahn, U. von Sacken and C. A. Michael, *Solid State Ionics* **44** (1990) 87.
[16] J. J. Auborn and Y. L. Barberio, *J. Electrochem. Soc.* **134** (1987) 638.
[17] E. Plicta, S. Slane, M. Uchiyama, M. Salomon, D. Chua, W. B. Ebner and H. W. Lin, *ibid.* **136** (1989) 1865.
[18] R. J. Gummow, D. C. Liles, M. M. Thackeray, *Mat. Res. Bull.* **28** (1993) 1249.
[19] B. Oyang, S. G. Greenbaum, M. Boer, A. Massucco, M. McLin, J. Shi and D. Fauteux, *Mat. Res. Proc.* **369** (1995) 29.
[20] H. M. Rietveld, *J. Appl. Cryst.* **2** (1969) 65.
[21] A. C. Larson and R. B. von Dreele, LANCE, MS-H805, Los Alamos National Laboratory, Los Alamos, NM (1995).
[22] Y. Gao and J. R. Dahn, *Appl. Phys. Lett.* **66** (1995) 2487.
[23] National Bureau of Standards (US), 'Monograph 25', **21** (1984) 78.
[24] A. Mosbah, A.Verbaere and M. Tournoux, *Mat. Res. Bull.* **18** (1983) 1375.
[25] W. D. Johnston, R. R. Heikes and D. Sestrich, *J. Phys. Chem. Sol.* **7** (1958) 1.
[26] D. Fauteux, A. Massucco, M. Rona and K. Johnson, Proc. 8th Lithium Battery Meeting, Japan, June (1996).